Title	A dual-color marker system for in vivo visualization of cell cycle progression in Arabidopsis
Author(s)	Ke Yin, Minako Ueda, Hitomi Takagi, Takehiro Kajihara, Shiori Sugamata Aki, Takashi Nobusawa, Chikage Umeda - Hara, Masaaki Umeda
Citation	The Plant Journal, 80(3):541-552
Issue Date	27 August 2014
Resource Version	Author
Rights	© 2014 The Authors The Plant Journal © 2014 John Wiley & Sons Ltd This is the peer reviewed version of the following article: [The Plant Journal, 80(3):541-552], which has been published in final form at [https://doi.org/10.1111/tpj.12652]. This article may be used for non-commercial purposes in accordance with Wiley Terms and Conditions for Use of Self-Archived Versions.
DOI	10.1111/tpj.12652
URL	http://hdl.handle.net/10061/12589

A dual-color marker system for *in vivo* visualization of cell cycle progression in *Arabidopsis*

Ke Yin[1],*, Minako Ueda[1],*, Hitomi Takagi[1], Takehiro Kajihara[1], Shiori Sugamata Aki[1], Takashi Nobusawa[1], Chikage Umeda-Hara[1] and Masaaki Umeda[1,2]

[1]Graduate School of Biological Sciences, Nara Institute of Science and Technology, Takayama 8916-5, Ikoma, Nara 630-0192, Japan; [2]JST, CREST, Takayama 8916-5, Ikoma, Nara 630-0192, Japan

*These authors contributed equally to the article.

For correspondence: Masaaki Umeda (Graduate School of Biological Sciences, Nara Institute of Science and Technology, Takayama 8916-5, Ikoma, Nara 630-0192, Japan; Tel. +81-743-72-5592; Fax +81-743-72-5599; E-mail: mumeda@bs.naist.jp)

Authors' email addresses: Ke Yin (kekeyin@gmail.com), Minako Ueda (m-ueda@itbm.nagoya-u.ac.jp), Hitomi Takagi (ask.microfin@gmail.com), Takehiro Kajihara (takehiro6021@gmail.com), Shiori Sugamata Aki (aki@bs.naist.jp), Takashi Nobusawa (tea.nobusawa@gmail.com), Chikage Umeda-Hara (chara@bs.naist.jp), Masaaki Umeda (mumeda@bs.naist.jp)

Running title: *In vivo* imaging of the cell cycle

Keywords: Cell cycle, real-time imaging, fluorescent protein marker, endocycle, *Arabidopsis thaliana*

Word count: 5876 (247 for Summary, 639 for Introduction, 2304 for Results, 1226 for

Discussion, 601 for Experimental Procedures, 77 for Acknowledgements, 782 for Figure

Legends), and 1796 for References

Present address

Minako Ueda: Institute of Transformative Bio-Molecules (ITbM), Nagoya University,

Furo-cho, Chikusa-ku, Nagoya, Aichi 464-8402, Japan

Takashi Nobusawa: Center for Biological Resources and Informatics, Tokyo Institute of

Technology, 4259 Nagatsuta-cho, Midori-ku, Yokohama 226-8501, Japan

2

Summary

Visualization of the spatiotemporal pattern of cell division is crucial to understanding how multicellular organisms develop and how they modify their growth in response to varying environmental conditions. The mitotic cell cycle consists of four phases: S (DNA replication), M (mitosis and cytokinesis), and the intervening G1 and G2 phases; however, only G2/M-specific markers are currently available in plants, making it difficult to measure cell cycle duration and to analyze changes in cell cycle progression in living tissues. Here, we developed another cell cycle marker that labels S-phase cells by manipulating *Arabidopsis CDT1a*, which functions in DNA replication origin licensing. Truncations of the *CDT1a* coding sequence revealed that its carboxy-terminal region is responsible for proteasome-mediated degradation at late G2 or in early mitosis. We therefore expressed this region as an RFP fusion protein under the S-specific promoter of a histone 3.1-type gene, *HISTONE THREE RELATED2* (*HTR2*), to generate an S/G2 marker. Combining this marker with the G2/M-specific *CYCB1-GFP* marker enabled us to visualize both S-to-G2 and G2-to-M cell cycle stages, and thus yielded an essential tool for time-lapse imaging of cell cycle progression. The resultant dual-color marker system, Cell-Cycle Tracking in Plant Cells (Cytrap), also allowed us to identify root cells in the last mitotic cell cycle before they entered the endocycle. Our results demonstrate that Cytrap is a powerful tool for *in vivo* monitoring of the plant cell cycle, and thus for deepening our understanding of cell cycle regulation in particular cell types during organ development.

Introduction

Monitoring the cell cycle in living tissues is a precise and direct way to understand how cell division is controlled in multicellular organisms. To visualize cell cycle progression in living cells, it is essential to develop appropriate markers by fusing fluorescent proteins to particular proteins that display cell cycle phase-specific accumulation. For example, the cell cycle marker 'Fucci' was developed in mouse, human and zebrafish, and is widely used in diverse research areas including studies on organ formation, cancer cell trafficking and embryogenesis (Sakaue-Sawano *et al*., 2008; Sugiyama *et al*., 2009). In the Fucci marker, S/G2/M-specific Geminin and G1/S-specific Cdt1 sequences are fused to green and red fluorescent proteins (GFP and RFP), respectively (Sakaue-Sawano *et al*., 2008; Sugiyama *et al*., 2009). This dual marker system makes it possible to identify the duration of the cell cycle and phase-specific changes in cell cycle progression. However, in plants, only G2/M-specific marker genes are currently available; examples include GUS- or GFP-fused B1-type cyclins (*CYCB1;1* and *CYCB1;2*) and plant-specific B2-type cyclin-dependent kinase (*CDKB2*) (Colon-Carmona *et al*., 1999; Ubeda-Tomás *et al*., 2009; Adachi *et al*., 2006; Iwata *et al*., 2011). Thus, the development of at least one more marker that visualizes cell cycle stage(s) other than G2/M is prerequisite for monitoring cell cycle progression in living plant tissues.

In *Arabidopsis*, several genes whose transcripts are elevated in G1 and/or S phase have been identified, such as those encoding D-type cyclins and histones (Menges *et al*., 2005; Okada *et al*., 2005; Dewitte *et al*., 2007; Takahashi *et al*., 2010). However,

their products are not targeted for cell cycle phase-specific proteolysis, and therefore persist after transcription ceases (Fang and Spector, 2005; Boudolf *et al*., 2009). This renders these genes unsuitable as G1/S- or S-phase markers, which need to display apparent switching on and off in each round of the cell cycle. Eukaryotic Cdt1 is an essential loading factor that enables the MCM helicase to associate with and activate DNA replication origins (for reviews, see Blow and Dutta, 2005; Machida and Dutta, 2005). For each round of DNA replication, the MCM helicase is released from DNA to avoid a second round of replication; thus, Cdt1 is tightly controlled during the cell cycle by being exported from the nucleus in budding yeast or by phase-specific proteolysis in other eukaryotes (Nishitani *et al*., 2000; Nishitani *et al*., 2001; Tanaka and Diffley, 2002). Such cell cycle-dependent regulation of protein accumulation made Cdt1 a successful G1/S-phase reporter in the Fucci marker (Sakaue-Sawano *et al*., 2008; Sugiyama *et al*., 2009). In *Arabidopsis*, two homologous genes, *CDT1a* and *CDT1b,* have been identified (Masuda *et al*., 2004). The *cdt1a* mutant shows a partially gametophytic-lethal phenotype, and this lethality is enhanced when *cdt1a* is combined with the *cdt1b* mutation (Domenichini *et al*., 2012); silencing of both *CDT1a* and *CDT1b* inhibited nuclear DNA replication and plastid division (Raynaud *et al*., 2005). Ectopic expression of *CDT1a* enhanced endoreplication, indicating another function in DNA polyploidization (Castellano *et al*., 2004). *CDT1a* expression is regulated by the transcription factor E2F, and the mRNA level decreases when plants are exposed to dehydration or abscisic acid treatment (Castellano *et al*., 2004). Furthermore, its protein level is controlled by proteasomal degradation, which is triggered by CDK

phosphorylation (Castellano *et al*., 2004). Collectively, these properties suggest that CDT1a would be an effective S-phase marker.

In this study, we tested whether *Arabidopsis CDT1a* could be exploited to generate a new cell cycle marker. We found that the C-terminal region of CDT1a is necessary and sufficient to promote proteolysis at late G2 or in early mitosis. An RFP fusion protein including this region of CDT1a and expressed under the histone 3.1-type gene promoter accumulated from S to G2, and we therefore combined it with the G2/M-specific *CYCB1;1-GFP* reporter. The resultant dual-color marker system was useful for time-lapse imaging of the cell cycle in the root meristem.

Results

Proteasomal degradation controls CDT1a accumulation during the cell cycle

To determine whether *Arabidopsis CDT1a* would be a suitable S-phase marker, we first examined accumulation of ß-glucuronidase (GUS)-fused CDT1a in seedlings. When a genomic fragment containing the 1.9-kb promoter and 2.5-kb protein-coding region was fused to the *GUS* gene (*pCDT1a::CDT1a-GUS*; Figure 2a), we observed patchy patterns of signals in proliferating tissues such as the root meristem, young leaves and emerging lateral roots (Figure 1a-c,e and Figure 2b). The GUS signal was also detected in endoreplicating tissues, such as trichomes and the elongation/differentiation zone (EDZ) of roots (Figure 1d and Figure 2b) (Takatsuka and Umeda, 2014). Notably, the number of GUS spots was lower in actively dividing cells in the root meristem than in endoreplicating cells in the EDZ (Figure 2b). When the promoter region alone was

fused to *GUS* (*pCDT1a::GUS*; Figure 2a), it yielded a uniform expression pattern as reported previously (Castellano *et al*., 2004) (Figure 1f-j and Figure 2c). These results suggest that post-transcriptional regulation is involved in the control of CDT1a protein accumulation.

To test the involvement of proteasome-mediated protein degradation, we treated the reporter lines with carbobenzoxylleucinyl-leucinyl-leucinal-H (MG132), an effective proteasome inhibitor in both animals and plants (Rock *et al*., 1994; Genschik *et al*., 1998). When *pCDT1a::CDT1a-GUS* seedlings were grown in the presence of MG132 for 4 h, GUS-positive cells in the root tip became more numerous, and the signals more intense, than in the DMSO-treated control (Figure 3b). *pCDT1a::GUS* lines showed no such increase in GUS signals (Figure 3a). This experiment indicates that CDT1a level is under the control of proteasomal degradation, and that this regulation is required for cell cycle stage-specific accumulation and destruction, which is manifested in the patchy pattern of GUS signals.

The carboxy-terminal half of CDT1a is sufficient for proteasome-dependent proteolysis

A previous study showed that ectopic expression of *CDT1a* in *Arabidopsis* caused various abnormal phenotypes, such as increased DNA ploidy, more trichome branches and higher stomatal density (Castellano *et al*., 2004). To eliminate the potential for exhibiting such undesirable phenotypes from the cell cycle marker, we tested a series of reporter genes with truncations in the coding region. CDT1a contains copies of two

hallmarks of protein degradation (Figure 2a). One is three minimal destruction boxes (D-boxes; RxxL), at amino acid positions 220, 396 and 555 from the start codon, which are required for ubiquitination by an E3 ligase, anaphase-promoting complex/cyclosome (APC/C) (Glotzer *et al.*, 1991; for a review, see King *et al.*, 1996). The other one is two PEST motifs, at amino acid positions 380 and 411, which are rich in proline, glutamic acid, serine and threonine residues (for a review, see Rechsteiner and Rogers, 1996). We also found three cyclin-binding motifs (Cy motifs), at amino acid positions 176, 372 and 397, which are required for phosphorylation by CDK, and in some cases, for subsequent degradation via the E3 ubiquitin ligase SCF[Skp2] (Nishitani *et al.*, 2006; Sugimoto *et al.*, 2004). Since most of these motifs are located in the carboxy (C)-terminal half of CDT1a (Figure 2a), we focused on this region for testing the suitability of CDT1a as a cell cycle marker.

When this C-terminal region of amino acid positions 285-571 (corresponding to nucleotide positions 1344-2505 from the start codon) was fused to GUS, we observed a patchy pattern of signals localized mainly in the root meristem (Figure 2a,d; *pCDT1a::CDT1a (C1)-GUS*). However, a further deletion of amino acid positions 456-571 (nucleotide positions 1983-2505) made the GUS signal weaker and fuzzy, probably due to a partial loss of regulatory sequences required for cell cycle stage-specific degradation (Figure 2a,e; *pCDT1a::CDT1a (C2)-GUS*). We then tested the region of amino acid positions 363-571 (nucleotide positions 1578-2505), and found that this reporter exhibited stronger signals in the meristem and in the distal region of the EDZ (Figure 2a,f; *pCDT1a::CDT1a (C3)-GUS*). Since *pCDT1a::CDT1a (C1)-GUS* and

pCDT1a::CDT1a (C3)-GUS showed a clear patchy signal pattern, we examined whether protein accumulation is enhanced by MG132 treatment. As expected, both GUS fusion proteins accumulated to high levels when the reporter lines were grown in the presence of 50 μM MG132 for 4 h (Figure 3c,d). These results indicate that GUS-fused CDT1a (C1) and CDT1a (C3) retain the capacity to be degraded via the ubiquitin-proteasome pathway in a cell cycle stage- specific manner. As mentioned above, full-length CDT1a accumulated to a lesser extent in the meristem than in the EDZ; however, we observed more intense GUS signals in the meristem expressing *CDT1a (C1)-GUS* or *CDT1a (C3)-GUS* than in that expressing full-length CDT1a (Figure 2b,d,f). This suggests that the regulatory element restraining higher CDT1a accumulation in actively dividing cells resides in the N-terminal half, and is missing in CDT1a (C1) and CDT1a (C3).

CDT1a (C3) is not functional in yeast and plant cells

We then examined whether the truncated CDT1a proteins retain their function in DNA replication. The temperature-sensitive *cdt1* mutant of *Saccharomyces cerevisiae*, *cdt1-td*, can grow at 24°C, but not at 37°C (Tanaka and Diffley, 2002; Figure 4a). When yeast *Cdt1* or the full-length cDNA of *Arabidopsis CDT1a* was expressed in *cdt1-td* using the galactose/tetracycline-inducible gene expression system (Belli *et al.*, 1998), the temperature sensitivity was fully suppressed (Figure 4a). In contrast, cDNAs encoding CDT1a (C1) or CDT1a (C3) displayed only weak or no complementation activity (Figure 4a), suggesting that these truncated proteins lack the full-length CDT1a function that depends on the central domain, which is required for the interaction with MCM

proteins (Yanagi *et al*., 2002).

Since *CDT1a* overexpression is known to increase the nuclear DNA content in plants (Castellano *et al*., 2004), we measured the DNA ploidy in leaves expressing *CDT1a (C3)*. In the wild-type, young leaves mainly possess 2C and 4C nuclei, and higher DNA ploidy (8C and 16C) appears during maturation (Figure 4b) (Galbraith *et al*., 1991). The profiles observed in leaves expressing *CDT1a (C3)-GUS* were similar to those in the wild-type (Figure 4b), whereas Castellano *et al*. (2004) reported that the proportion of 8C and 16C nuclei was significantly higher in plants overexpressing full-length *CDT1a* than in the wild-type. In summary, CDT1a (C3) exhibited stronger GUS expression than CDT1a (C1) (Figure 2d,f), and was non-functional in yeast and probably also in plant cells (Figure 4a,b); thus, we hereafter focused on CDT1a (C3) to generate a cell cycle marker. Similar to the full-length version (*pCDT1a::CDT1a-GUS*), *pCDT1a::CDT1a (C3)-GUS* exhibited GUS expression in proliferating tissues, such as shoot and root meristems, expanding young leaves and emerging lateral roots (Figure S1).

***CDT1a* promoter-driven *CDT1a (C3)* marks the S-to-G2 phase in tobacco BY-2 cells**

Next, to determine the cell cycle stage at which the CDT1a (C3)-GUS fusion protein accumulates, we introduced *pCDT1a::CDT1a (C3)-GUS* into cultured tobacco Bright Yellow-2 (BY-2) cells. Transformed cells were synchronized with aphidicolin at early S phase (Breyne *et al*., 2002), and cell cycle progression was monitored after aphidicolin

release by measuring the mitotic index and DNA content using a flow cytometer. Our measurement of GUS activity showed that the peak of CDT1a (C3)-GUS accumulation correlated well with that of S-phase cells (Figure 5a,b). However, synchronization by aphidicolin does not give a high percentage of S-phase cells in the second round of the cell cycle due to incomplete synchrony of the cell culture (Figure 5b); therefore, to precisely define the cell cycle stage at which CDT1a (C3)-GUS accumulates, we conducted a two-step synchronization with aphidicolin and propyzamide, which permits synchronous progression from M (prometaphase) after release from the propyzamide block (Nagata *et al.*, 1992). The GUS activity started to increase 6 h after propyzamide release, when the number of S-phase cells also began to increase (Figure 5c,d). This suggests that the *CDT1a* promoter functions from the beginning of the S phase. A reduction of GUS activity and S-phase cell number began to occur between 10 and 11 h, but the initial decline in GUS activity was less sharp than that of S-phase cell number (Figure 5c,d). This indicates that CDT1a (C3)-GUS continues to accumulate when the cells exit the S phase.

The *HTR2* promoter increases the fluorescence intensity of the S/G2 marker

To develop an effective time-lapse imaging marker, we replaced GUS with GFP to generate *pCDT1a::CDT1a (C3)-GFP*. As shown in Figure 6a, it exhibited a patchy pattern of GFP signals in the root tip, but the fluorescence intensity was very weak. The GFP marker carrying the full-length *CDT1a* cDNA also showed very faint signals (*pCDT1a::CDT1a-GFP*; Figure 6b), suggesting that the *CDT1a* promoter exerts

relatively low transcription activity *in planta*. These results prompted us to test the promoter of histone H3.1-type gene *HISTONE THREE RELATED2* (*HTR2*) (At1g09200), which shows S phase-specific expression with a higher transcript level in young organs (Okada *et al.*, 2005). We found that *pHTR2::HTR2-GFP* displayed higher GFP fluorescence than *pCDT1a::CDT1a-GFP* (Figure 6b,c). However, the GFP signal was visible in mitotic cells with segregating daughter chromosomes (Figure 6c, inset), indicating that HTR2-GFP accumulation persists into M phase. We then replaced the coding region of *HTR2* with *CDT1a (C3)* to trigger active protein degradation. The resultant *pHTR2::CDT1a (C3)-GFP* marker showed markedly higher fluorescence than *pCDT1a::CDT1a (C3)-GFP* (Figure 6d; compare to Figure 6a). The GFP signal was never detected in cells with mitotic figures (Figure 6d; compare to Figure 6c), supporting the idea that CDT1a (C3)-GFP is degraded before metaphase. The expression pattern was similar to the staining pattern with 5-ethynyl-2'-deoxyuridine (EdU), which is incorporated into replicating DNA (Figure 6e) (Salic and Mitchison, 2008), suggesting the validity of *pHTR2::CDT1a (C3)-GFP* as a monitor of S-phase progression. We noticed that GFP fluorescence often appeared in consecutive cells in a particular cell file (Figure 6d), indicating synchronous cell division in the same cell lineage. Hayashi *et al.* (2013) recently made a similar observation using EdU incorporation to visualize root cells undergoing DNA replication.

Dual-color time-lapse imaging can monitor the whole cell cycle stages

To make a reporter system monitoring the whole cell cycle stages, we replaced GFP

with RFP to generate *pHTR2::CDT1a (C3)-RFP*. This S/G2 marker was introduced into *Arabidopsis* together with the G2/M marker *pCYCB1::CYCB1-GFP*, which carries the promoter and the N-terminal region of *CYCB1;1*, allowing protein degradation through the D-box (Ubeda-Tomás *et al*., 2009; Figure 6f). In the root meristem, we could observe all four fluorescence combinations, i.e., no fluorescence, either RFP (Figure 6g) or GFP (Figure 6h), and both RFP and GFP fluorescence (Figure 6i), presumably representing G1, S-G2, G2-M and G2 phases, respectively. The DNA ploidy profiles in leaves expressing both reporter genes were similar to those in the wild-type (Figure S2), suggesting that a higher expression of *CDT1a (C3)-RFP* under the control of *HTR2* promoter did not affect endoreplication.

To precisely assign each fluorescence signal to a particular stage of the cell cycle, we performed *in vivo* time-lapse imaging of epidermal cells in the root meristem (Colon-Carmona *et al*., 1999; Campilho *et al*., 2006). Time-lapse imaging for 14 h with 10-min intervals enabled us to trace changes in fluorescence intensity (Movie S1). The GFP signal of *pCYCB1::CYCB1-GFP* was evident on the equatorial plane in mitotic cells (metaphase), but it rapidly disappeared when the sister chromatids began to separate (anaphase) (Figure 7a). To provide a timescale, the time point at which the equatorial plane was transiently visualized by GFP signals was therefore set to zero (Figure 7a,c). We found that the GFP signal appeared at -3 h, when the RFP signal of *pHTR2::CDT1a (C3)-RFP* was still detectable. Both GFP and RFP signals were observed for the next 1 h, after which GFP fluorescence alone was detected for 2 h until metaphase (Figure 7a,c and Figure 8).

Previous reports suggested that the duration of the cell cycle in *Arabidopsis* roots is around 17 h (Cools *et al*., 2010; Hayashi *et al*., 2013). However, in our imaging system, 14 h was the maximum observation period due to cellular damage caused by the laser; thus, we could not monitor the whole cell cycle solely on the GFP-based timescale (Figure 7c). We therefore set another timescale: the time point at which the intensity of RFP signals first exceeded twice the value detected 2 h previously was set to zero (Figure 7b,d). Our observation revealed that the RFP signal appeared 6 h after disappearance of the GFP signal at anaphase, and that it persisted for 8 h (Figure 7b,d). These results indicate that GFP- and RFP-based measurements can track the whole cell cycle; namely, 6 h from M (anaphase) to G1, 8 h from S to G2, and 3 h from late G2 to M (metaphase) in which the first hour is an overlap between the RFP and GFP signals in G2 (and early M) (Figure 8). We designated this dual-color marker system as Cell-Cycle Tracking in Plant Cells (Cytrap).

In *Arabidopsis* root tips, dividing cells enter the endocycle around the transition zone (TZ), which is located between the meristematic zone and the EDZ (Figure 9a), and start to increase cell length (cell volume) and DNA content (De Veylder *et al*., 2011; Takatsuka and Umeda, 2014; Edgar *et al*., 2014). We observed root cortical cells around the TZ in the Cytrap line. The GFP fluorescence of *pCYCB1::CYCB1-GFP* was not detected at all in this region (Figure 9a), which is consistent with an existing idea that the whole M phase is skipped in the endocycle (for a review, see Joubes and Chevalier, 2000). Instead, the RFP signal of *pHTR2::CDT1a (C3)-RFP* was observed throughout the TZ, and it was also detected in 4.0 ± 2.1 (mean ± s.d., n=15) cells

preceding the first TZ cell, which can be identified by a sudden increase in cell size (Figure 9b) (for a review, see Verbelen *et al*., 2006). We infer that the four RFP-expressing cells preceding the TZ are in the S-to-G2 phase of the last mitotic cell cycle, thus possessing a DNA content of 4C. This result indicates that cell expansion occurs after the decision to commit to the endocycle has been made in S/G2-phase cells preceding the TZ.

Discussion

Regulation of CDT1a accumulation in *Arabidopsis*

In this study, we revealed that the C-terminal region of *Arabidopsis* CDT1a is responsible for proteasomal degradation, which prevents CDT1a from persisting through mitosis. In the vertebrate Fucci system, the G1/S-specific marker Cdt1 accumulates by the end of S phase (Sugimoto *et al*., 2004; Sakaue-Sawano *et al*., 2008), implying that Cdt1 protein stability is differentially controlled among various organisms. This idea is consistent with the fact that the C-terminal region of *Arabidopsis* CDT1a, which carries multiple hallmarks of protein degradation (Figure 2a), is highly divergent from that of its orthologs in other eukaryotes. Sugiyama *et al*. (2009) found that the mammalian Cdt1 reporter is not functional in zebrafish, probably because it is not ubiquitinated properly by a fish E3 ubiquitin ligase. This implies that the degradation machinery is also divergent among different organisms.

Our synchronization experiments with tobacco BY-2 cells showed that the *CDT1a* promoter is activated at the beginning of S phase (Figure 5). However,

transcription of yeast *Cdt1* starts from G1 (Hofmann and Beach, 1994), and the mRNA

level of human *Cdt1* does not change dramatically during the cell cycle (Nishitani *et al*.,

2001). Therefore, transcriptional regulation of *Cdt1* also differs between plants and

other eukaryotes. Due to the low promoter activity of *Arabidopsis CDT1a*, we replaced

the promoter region in the reporter gene with that of *HTR2*, which is highly expressed

from the beginning of S phase (Okada *et al*., 2005). Promoters of other S-phase genes

should be also useful, such as those driving expression of the core histones, which are

transcribed and incorporated into nucleosomes at different times during DNA

replication (Cools *et al*., 2010). Moreover, tissue-specific S-phase promoters are

potentially powerful tools to analyze particular developmental processes; for instance,

the promoter of male gamete-specific *HISTONE3.3* may be useful for testing the

hypothesis that male gametes are arrested at S and proceed to G2 just before

fertilization (Friedman, 1999; Ingouff *et al*., 2007; for a review, see Lord and Russell,

2002), and for examining whether the central cell and the egg cell are in a similar cell

cycle phase during fertilization.

***In vivo* visualization of the cell cycle**

Time-lapse imaging of epidermal cells in the root meristem revealed that

pHTR2::CDT1a (C3)-RFP and *pCYCB1::CYCB1-GFP* are expressed for approximately

8 and 3 h, respectively, with an overlapping period of 1 h. *pCYCB1::CYCB1-GFP* is

known to be expressed from the late G2 (Colon-Carmona *et al*., 1999), and our analysis

showed that the CYCB1-GFP fusion protein was rapidly degraded as cells entered

anaphase (Figure 7a). This means that *pHTR2::CDT1a (C3)-RFP* marks the period from

S to late G2 or early M (8 h), and *pCYCB1::CYCB1-GFP* from late G2 to metaphase (3

h) (Figure 8). Our analysis also revealed that there was a period of 6 h showing no

fluorescence (Figure 7d). Considering that anaphase, telophase and cytokinesis occur

rapidly (Kurihara *et al*., 2008), 6 h is the likely approximate duration of G1 (Figure 8).

Counting the 1-h overlap in expression of the two fluorescence markers, the cell cycle

duration is estimated to be 16 h. This is consistent with a previous estimate of 17 h,

which was based on gene expression profiles in *Arabidopsis* roots synchronized with

hydroxyurea (Cools *et al*., 2010). Hayashi *et al*. (2013) recently measured cell cycle

progression in *Arabidopsis* roots by EdU incorporation; they reported that the duration

of the cell cycle was 17.1 h, with that of S-phase being 2.9 h, in the meristematic zone.

Assuming that the S-phase duration is 3 h in our imaging analysis, the 16-h cycle

consequently consists of 6 h of G1, 3 h of S, 5 h of G2, and 2 h of M.

We noticed that the maximum duration of our time-lapse imaging using a

confocal microscope was 14 h, implying that it is impossible to trace the whole round of

the cell cycle. This limitation is likely due to a reduction in cell division activity caused

by prolonged confocal laser irradiation and unfavorable root growth under dark

conditions; indeed, the RFP signal displayed a sharp peak when the timescale was based

on the RFP fluorescence (Figure 7d), whereas it did not increase so sharply when

images were captured for more than 10 h after the onset of GFP fluorescence (Figure

7c). Technical improvement of the imaging system, perhaps by using multi-photon

confocal microscopy in a light growth chamber (for a review, see Niesner and Hauser,

2011), will therefore be required for real-time monitoring of the whole cell cycle in living tissues. We also noticed that *pCYCB1::CYCB1-GFP* yielded relatively weak signals, and a much brighter G2/M-phase reporter would be beneficial to the Cytrap system. Many *Arabidopsis* genes showing G2/M-specific expression have been identified, such as mitotic cyclins, B2-type CDKs and cytokinesis-related genes (Menges *et al*., 2003; Haga *et al*., 2007; Kato *et al*., 2009; Iwata *et al*., 2011), and we anticipate that one or more of these would be a better G2/M-marker in the Cytrap system.

Our observations revealed that *pHTR2::CDT1a (C3)-RFP* was expressed in the 4-5 consecutive cells preceding the first elongated TZ cell, as well as in all TZ cells. This result implies that cell enlargement occurs after progression through S/G2 of the last mitotic cell cycle. We recently reported that *CCS52A1* promoter activity is absent in the meristem, but is induced a few cells before the first elongated TZ cell (Takahashi *et al*., 2013). *CCS52A1* encodes an activator of APC/C, which promotes the onset and progression of the endocycle through degradation of mitotic regulators, such as mitotic cyclins (Larson-Rabin *et al*., 2009). The expression pattern of *CCS52A1* around the TZ is very similar to that of *pHTR2::CDT1a (C3)-RFP*, demonstrating that the decision to enter the endocycle is made during the S-to-G2 phase of the last mitotic cell cycle, and is accompanied by APC/C-mediated destruction of mitotic regulators. The RFP signal of *pHTR2::CDT1a (C3)-RFP* was detected throughout the TZ and beyond the EDZ without the patchy pattern displayed in the meristematic zone (Figure 9a), indicating that CDT1a (C3)-RFP is not degraded after cells start endoreplication. This indicates

that, during endoreplication, DNA replication is followed by a gap phase in which CDT1a (C3)-RFP is not recognized by the degradation machinery that usually functions at the end of G2 or early M in the mitotic cell cycle. Because fluorescence signals of tdTomato-labeled histone H2B on chromosomes correlate well with the actual DNA level (Adachi *et al*., 2011), a fluorescent marker fused to histone H2B may be useful to measure the DNA level and monitor endocycle progression in the TZ.

Conclusion

A portion of the C-terminal region of CDT1a, named CDT1a (C3), was necessary and sufficient for proteasomal degradation at late G2 or in early mitosis. Consequently, when expressed under its own promoter, GFP-fused CDT1a (C3) specifically accumulated from S to G2. We expressed CDT1a (C3)-RFP under the strong S-phase promoter of *HTR2*, and combined this marker with the G2/M-specific reporter CYCB1-GFP to generate a dual-color marker system, which we named Cell-Cycle Tracking in Plant Cells (Cytrap). Time-lapse imaging with Cytrap allowed us both to monitor cell cycle progression in the root meristem and to label the last mitotic cell cycle before entry into the endocycle. Cytrap is an excellent and adaptable tool to visualize cell cycle progression in living plant tissues, and should be applicable to a variety of analyses involving cell division during organ formation and development.

Experimental Procedures

Plant materials and growth conditions

Arabidopsis thaliana (ecotype Col-0) was used as the wild-type. *pCYCB1::CYCB1-GFP* (Colon-Carmona *et al*., 1999; Ubeda-Tomás *et al*., 2009) and *pHTR2::HTR2-GFP* were provided by Drs. P. Doerner and D. Kurihara, respectively. Plant growth conditions and MG132 treatment were as described previously (Adachi *et al*., 2011).

Generation of transgenic lines

Plasmids were constructed using the Gateway system (Invitrogen, Carlsbad, CA, USA). For the GUS fusion series of *CDT1a*, the *CDT1a* promoter (1894 bp) was cloned into the Gateway pDONR-P4P1R vector, and the full-length *CDT1a* coding region (+1 to 2508) as well as *CDT1a (C1)* (+1344 to 2508), *CDT1a (C2)* (+1344 to 1983) and *CDT1a (C3)* (+1578 to 2508) were cloned into pDONR221 (Invitrogen). Each fragment was combined with the *CDT1a* promoter in the R4pGWB533 binary vector to create *pCDT1a::CDT1a-GUS*, *pCDT1a::CDT1a (C1)-GUS*, *pCDT1a::CDT1a (C2)-GUS* and *pCDT1a::CDT1a (C3)-GUS* (Nakagawa *et al*., 2008). The same method was used to make *pCDT1a::CDT1a-GFP* and *pCDT1a::CDT1a (C3)-GFP* in the *GFP*-carrying binary vector R4pGWB550 (Nakagawa *et al*., 2008). *pCDT1a::GUS* was made by cloning the *CDT1a* promoter into the *GUS*-carrying binary vector R4L1pGWB533 (Nakamura *et al*., 2009). For *pHTR2::CDT1a (C3)-GFP* and *pHTR2::CDT1a (C3)-RFP*, the *HTR2* promoter (1.1 kb) was fused to *CDT1a (C3)* in pDONR221, and *pHTR2-CDT1a (C3)* was cloned into pGWB550 (GFP) and pGWB401 (RFP), respectively (Nakagawa *et al*., 2009). The floral dip method was used to introduce these

constructs into Col-0 plants, except for generating the Cytrap marker, in which case *pHTR2::CDT1a (C3)-RFP* was introduced into *pCYCB1::CYCB1-GFP*-harboring plants (Clough and Bent, 1998).

Histochemical analysis

GUS and propidium iodide (PI) staining were performed as described by Adachi *et al.* (2011). EdU labeling was carried out using a Click-iT-EdU imaging kit (Invitrogen) according to the manufacturer's instruction. Fluorescence images of GFP, RFP, PI and EdU were taken with an Olympus FV1000 confocal microscope with FV10-ASW version 03.01 software, using a 40x/0.95-numerical aperture objective and argon 488-nm (GFP and EdU) and 559-nm (RFP and PI) laser lines (Olympus, Tokyo, Japan). FV10-ASW software was also used to measure the fluorescence intensity of the Cytrap marker in nuclei of epidermal cells.

Yeast complementation test

The yeast *cdt1-td* mutant (YST108) and a control plasmid expressing yeast *Cdt1* (pST283) were obtained from Dr. S. Tanaka (Tanaka and Diffley, 2002). cDNA fragments of *Arabidopsis CDT1a* were cloned into the pST517 vector, and introduced into YST108. A complementation assay was conducted as described by Tanaka and Diffley (2002).

DNA ploidy measurement

Ploidy distribution in leaves and BY-2 cells was measured with a ploidy analyzer PA (Partec) and CyStain UV precise P (Partec).

Synchronization of tobacco BY-2 cells

Maintenance, synchronization and *Agrobacterium tumefaciens*-mediated transformation of tobacco BY-2 cells were performed as described previously (Nagata *et al*., 1992; Nagata and Kumagai, 1999). The mitotic index and GUS activity were measured as described by Genschik *et al*. (1998) and Adachi *et al*. (2006), respectively.

In vivo **time-lapse imaging**

Arabidopsis seeds were germinated on a chambered cover glass (AGC TECHNO GLASS, Shizuoka, Japan), which contained 1.8 mL medium [0.5 × Murashige and Skoog salt mixture, 0.5 g/L 2-(N-morpholino) ethanesulfonic acid (MES) and 1% phytagel (Sigma, Tokyo, Japan), pH 5.8]. Plants were grown under continuous light conditions at 23°C. Five days after germination (DAG), epidermal cells in the region between 100 μm and 200 μm from the root tip were subjected to time-lapse imaging with an Olympus FV1000 confocal microscope. The system and acquisition settings were the same as those for histochemical analyses, except that a 20x/0.95-numerical aperture objective with 3.0x zoom was used. Two or three roots were observed simultaneously using FV10-ASW software, and images were collected at two different Z-positions every 10 min for 14 h.

Supporting Information

Figure S1. Expression pattern of *pCDT1a::CDT1a (C3)-GUS*.

Figure S2. DNA ploidy analysis of leaf cells of Cytrap transgenic lines.

Movie S1. Time-lapse imaging of a root harboring *pCYCB1::CYCB1-GFP* and *pHTR2::CDT1a (C3)-RFP*.

References

Adachi, S., Minamisawa, K., Okushima, Y., Inagaki, S., Yoshiyama, K., Kondou, Y., Kaminuma, E., Kawashima, M., Toyoda, T., Matsui, M., Kurihara, D., Matsunaga, S. and Umeda, M. (2011) Programmed induction of endoreduplication by DNA double-strand breaks in *Arabidopsis*. *Proc*. *Natl*. *Acad*. *Sci*. *USA*, **108**, 10004-10009.

Adachi, S., Uchimiya, H. and Umeda, M. (2006) Expression of B2-type cyclin-dependent kinase is controlled by protein degradation in *Arabidopsis thaliana*. *Plant Cell Physiol*. **47**, 1683-1686.

Belli, G., Gari, E., Aldea, M. and Herrero, E. (1998) Functional analysis of yeast essential genes using a promoter-substitution cassette and the tetracycline-regulatable dual expression system. *Yeast*, **14**, 1127-1138.

Blow, J.J. and Dutta, A. (2005) Preventing re-replication of chromosomal DNA. *Nat*. *Rev*. *Mol*. *Cell Biol*. **6**, 476-486.

Boudolf, V., Lammens, T., Boruc, J., Van Leene, J., Van Den Daele, H., Maes, S., Van Isterdael, G., Russinova, E., Kondorosi, E., Witters, E., De Jaeger, G., Inze, D. and De Veylder, L. (2009) CDKB1;1 forms a functional complex with CYCA2;3 to suppress endocycle onset. *Plant Physiol*. **150**, 1482-1493.

Breyne, P., Dreesen, R., Vandepoele, K., De Veylder, L., Van Breusegem, F., Callewaert, L., Rombauts, S., Raes, J., Cannoot, B., Engler, G., Inze, D. and Zabeau, M. (2002) Transcriptome analysis during cell division in plants. *Proc*. *Natl*. *Acad*. *Sci*. *USA*, **99**, 14825-14830.

Campilho, A., Garcia, B., Toorn, H.V., Wijk, H.V., Campilho, A. and Scheres, B. (2006) Time-lapse analysis of stem-cell divisions in the *Arabidopsis thaliana* root meristem. *Plant J*. **48**, 619-627.

Castellano, M.M., Boniotti, M.B., Caro, E., Schnittger, A. and Gutierrez, C. (2004) DNA replication licensing affects cell proliferation or endoreplication in a cell type-specific manner. *Plant Cell*, **16**, 2380-2393.

Clough, S.J. and Bent, A.F. (1998) Floral dip: a simplified method for *Agrobacterium*-mediated transformation of *Arabidopsis thaliana*. *Plant J*. **16**, 735-743.

Colon-Carmona, A., You, R., Haimovitch-Gal, T. and Doerner, P. (1999) Spatio-temporal analysis of mitotic activity with a labile cyclin-GUS fusion protein. *Plant J*. **20**, 503-508.

Cools, T., Iantcheva, A., Maes, S., Van den Daele, H. and De Veylder, L. (2010) A replication stress-induced synchronization method for *Arabidopsis thaliana* root meristems. *Plant J*. **64**, 705-714.

De Veylder, L., Larkin, J.C. and Schnittger, A. (2011) Molecular control and function of endoreplication in development and physiology. *Trends Plant Sci*. **16**, 624-634.

Dewitte, W., Scofield, S., Alcasabas, A.A., Maughan, S.C., Menges, M., Braun, N., Collins, C., Nieuwland, J., Prinsen, E., Sundaresan, V. and Murray, J.A. (2007) *Arabidopsis* CYCD3 D-type cyclins link cell proliferation and endocycles and are rate-limiting for cytokinin responses. *Proc. Natl. Acad. Sci.*

USA, **104**, 14537-14542.

Domenichini, S., Benhamed, M., De Jaeger, G., Van De Slijke, E., Blanchet, S., Bourge, M., De Veylder, L., Bergounioux, C. and Raynaud, C. (2012) Evidence for a role of *Arabidopsis* CDT1 proteins in gametophyte development and maintenance of genome integrity. *Plant Cell*, **24**, 2779-2791.

Edgar, B.A., Zielke, N. and Gutierrez, C. (2014) Endocycles: a recurrent evolutionary innovation for post-mitotic cell growth. *Nat. Rev. Mol. Cell Biol.* **15**, 197-210.

Fang, Y. and Spector, D.L. (2005) Centromere positioning and dynamics in living *Arabidopsis* plants. *Mol. Biol. Cell*, **16**, 5710-5718.

Friedman, W.E. (1999) Expression of the cell cycle in sperm of Arabidopsis: implications for understanding patterns of gametogenesis and fertilization in plants and other eukaryotes. *Development*, **126**, 1065-1075.

Galbraith, D.W., Harkins, K.R. and Knapp, S. (1991) Systemic endopolyploidy in *Arabidopsis thaliana*. *Plant Physiol.* **96**, 985-989.

Genschik, P., Criqui, M.C., Parmentier, Y., Derevier, A. and Fleck, J. (1998) Cell cycle -dependent proteolysis in plants: Identification of the destruction box pathway and metaphase arrest produced by the proteasome inhibitor MG132. *Plant Cell*, **10**, 2063-2076.

Glotzer, M., Murray, A.W. and Kirschner, M.W. (1991) Cyclin is degraded by the ubiquitin pathway. *Nature*, **349**, 132-138.

Haga, N., Kato, K., Murase, M., Araki, S., Kubo, M., Demura, T., Suzuki, K., Muller, I., Voss, U., Jurgens, G. and Ito, M. (2007) R1R2R3-Myb proteins

positively regulate cytokinesis through activation of *KNOLLE* transcription in *Arabidopsis thaliana*. *Development*, **134**, 1101-1110.

Hayashi, K., Hasegawa, J. and Matsunaga, S. (2013) The boundary of the meristematic and elongation zones in roots: endoreduplication precedes rapid cell expansion. *Sci. Rep.* **3**, 2723.

Hofmann, J.F. and Beach, D. (1994) cdt1 is an essential target of the Cdc10/Sct1 transcription factor: requirement for DNA replication and inhibition of mitosis. *EMBO J.* **13**, 425-434.

Ingouff, M., Hamamura, Y., Gourgues, M., Higashiyama, T. and Berger, F. (2007) Distinct dynamics of HISTONE3 variants between the two fertilization products in plants. *Curr. Biol.* **17**, 1032-1037.

Iwata, E., Ikeda, S., Matsunaga, S., Kurata, M., Yoshioka, Y., Criqui, M.C., Genschik, P. and Ito, M. (2011) GIGAS CELL1, a novel negative regulator of the anaphase-promoting complex/cyclosome, is required for proper mitotic progression and cell fate determination in *Arabidopsis*. *Plant Cell*, **23**, 4382-4393.

Joubes, J. and Chevalier, C. (2000) Endoreduplication in higher plants. *Plant Mol. Biol.* **43**, 735-745.

Kato, K., Galis, I., Suzuki, S., Araki, S., Demura, T., Criqui, M.C., Potuschak, T., Genschik, P., Fukuda, H., Matsuoka, K. and Ito, M. (2009) Preferential up-regulation of G2/M phase-specific genes by overexpression of the hyperactive form of NtmybA2 lacking its negative regulation domain in tobacco

BY-2 cells. *Plant Physiol*. **149**, 1945-1957.

King, R.W., Deshaies, R.J., Peters, J.M. and Kirschner, M.W. (1996) How proteolysis drives the cell cycle. *Science*, **274**, 1652-1659.

Kurihara, D., Matsunaga, S., Uchiyama, S. and Fukui, K. (2008) Live cell imaging reveals plant aurora kinase has dual roles during mitosis. *Plant Cell Physiol*. **49**, 1256-1261.

Larson-Rabin, Z., Li, Z., Masson, P.H. and Day, C.D. (2009) *FZR2/CCS52A1* expression is a determinant of endoreduplication and cell expansion in *Arabidopsis*. *Plant Physiol*. **149**, 874-884.

Lord, E.M. and Russell, S.D. (2002) The mechanisms of pollination and fertilization in plants. *Ann. Rev. Cell Dev. Biol*. **18**, 81-105.

Machida, Y.J. and Dutta, A. (2005) Cellular checkpoint mechanisms monitoring proper initiation of DNA replication. *J. Biol. Chem*. **280**, 6253-6256.

Masuda, H.P., Ramos, G.B., de Almeida-Engler, J., Cabral, L.M., Coqueiro, V.M., Macrini, C.M., Ferreira, P.C. and Hemerly, A.S. (2004) Genome based identification and analysis of the pre-replicative complex of *Arabidopsis thaliana*. *FEBS Lett*. **574**, 192-202.

Menges, M., de Jager, S.M., Gruissem, W. and Murray, J.A. (2005) Global analysis of the core cell cycle regulators of *Arabidopsis* identifies novel genes, reveals multiple and highly specific profiles of expression and provides a coherent model for plant cell cycle control. *Plant J*. **41**, 546-566.

Menges, M., Hennig, L., Gruissem, W. and Murray, J.A. (2003) Genome-wide gene

expression in an *Arabidopsis* cell suspension. *Plant Mol. Biol.* **53**, 423-442.

Nagata, T. and Kumagai, F. (1999) Plant cell biology through the window of the highly synchronized tobacco BY-2 cell line. *Methods Cell Sci.* **21**, 123-127.

Nagata, T., Nemoto, Y. and Hasezawa, S. (1992) Tobacco BY-2 cell line as the "HeLa" cell in the cell biology of higher plants. *Int. Rev. Cytol.* **132**, 1-30.

Nakagawa, T., Ishiguro, S. and Kimura, T. (2009) Gateway vectors for plant transformation. *Plant Biotechnol.* **26**, 275-284.

Nakagawa, T., Nakamura, S., Tanaka, K., Kawamukai, M., Suzuki, T., Nakamura, K., Kimura, T. and Ishiguro, S. (2008) Development of R4 gateway binary vectors (R4pGWB) enabling high-throughput promoter swapping for plant research. *Biosci. Biotechnol. Biochem.* **72**, 624-629.

Nakamura, S., Nakao, A., Kawamukai, M., Kimura, T., Ishiguro, S. and Nakagawa, T. (2009) Development of gateway binary vectors, R4L1pGWBs, for promoter analysis in higher plants. *Biosci. Biotechnol. Biochem.* **73**, 2556-2559.

Niesner, R.A. and Hauser, A.E. (2011) Recent advances in dynamic intravital multi-photon microscopy. *Cytometry,* **79**, 789-798.

Nishitani, H., Lygerou, Z., Nishimoto, T. and Nurse, P. (2000) The Cdt1 protein is required to license DNA for replication in fission yeast. *Nature*, **404**, 625-628.

Nishitani, H., Sugimoto, N., Roukos, V., Nakanishi, Y., Saijo, M., Obuse, C., Tsurimoto, T., Nakayama, K.I., Nakayama, K., Fujita, M., Lygerou, Z. and Nishimoto, T. (2006) Two E3 ubiquitin ligases, SCF-Skp2 and DDB1-Cul4, target human Cdt1 for proteolysis. *EMBO J.* **25**, 1126-1136.

Nishitani, H., Taraviras, S., Lygerou, Z. and Nishimoto, T. (2001) The human licensing factor for DNA replication Cdt1 accumulates in G1 and is destabilized after initiation of S-phase. *J. Biol. Chem.* **276**, 44905-44911.

Okada, T., Endo, M., Singh, M.B. and Bhalla, P.L. (2005) Analysis of the histone H3 gene family in *Arabidopsis* and identification of the male-gamete-specific variant AtMGH3. *Plant J.* **44**, 557-568.

Raynaud, C., Perennes, C., Reuzeau, C., Catrice, O., Brown, S. and Bergounioux, C. (2005) Cell and plastid division are coordinated through the prereplication factor AtCDT1. *Proc. Natl. Acad. Sci. USA*, **102**, 8216-8221.

Rechsteiner, M. and Rogers, S.W. (1996) PEST sequences and regulation by proteolysis. *Trends Biochem. Sci.* **21**, 267-271.

Rock, K.L., Gramm, C., Rothstein, L., Clark, K., Stein, R., Dick, L., Hwang, D. and Goldberg, A.L. (1994) Inhibitors of the proteasome block the degradation of most cell proteins and the generation of peptides presented on MHC class I molecules. *Cell*, **78**, 761-771.

Sakaue-Sawano, A., Kurokawa, H., Morimura, T., Hanyu, A., Hama, H., Osawa, H., Kashiwagi, S., Fukami, K., Miyata, T., Miyoshi, H., Imamura, T., Ogawa, M., Masai, H. and Miyawaki, A. (2008) Visualizing spatiotemporal dynamics of multicellular cell-cycle progression. *Cell*, **132**, 487-498.

Salic, A. and Mitchison, T.J. (2008) A chemical method for fast and sensitive detection of DNA synthesis *in vivo*. *Proc. Natl. Acad. Sci. USA*, **105**, 2415-2420.

Sugimoto, N., Tatsumi, Y., Tsurumi, T., Matsukage, A., Kiyono, T., Nishitani, H.

and Fujita, M. (2004) Cdt1 phosphorylation by cyclin A-dependent kinases negatively regulates its function without affecting geminin binding. *J. Biol. Chem.* **279**, 19691-19697.

Sugiyama, M., Sakaue-Sawano, A., Iimura, T., Fukami, K., Kitaguchi, T., Kawakami, K., Okamoto, H., Higashijima, S. and Miyawaki, A. (2009) Illuminating cell-cycle progression in the developing zebrafish embryo. *Proc. Natl. Acad. Sci. USA*, **106**, 20812-20817.

Takahashi, H., Yanamoto, S., Yamada, S., Umeda, M., Shigeta, T., Minamikawa, T., Shibuya, Y., Komori, T., Shiraishi, T., Asahina, I., Yokoo, S. and Ri, S. (2014) Effects of postoperative chemotherapy and radiotherapy on patients with squamous cell carcinoma of the oral cavity and multiple regional lymph node metastases. *Int. J. Oral Maxillofac. Surg.* **43,** 680-685.

Takahashi, I., Kojima, S., Sakaguchi, N., Umeda-Hara, C. and Umeda, M. (2010) Two *Arabidopsis* cyclin A3s possess G1 cyclin-like features. *Plant Cell Rep.* **29**, 307-315.

Takatsuka, H. and Umeda, M. (2014) Hormonal control of cell division and elongation along differentiation trajectories in roots. *J. Exp. Bot.* doi: 10.1093/jxb/ert485.

Tanaka, S. and Diffley, J.F. (2002) Interdependent nuclear accumulation of budding yeast Cdt1 and Mcm2-7 during G1 phase. *Nat. Cell Biol.* **4**, 198-207.

Ubeda-Tomás, S., Federici, F., Casimiro, I., Beemster, G.T.S., Bhalerao, R., Swarup, R., Doerner, P., Haseloff, J. and Bennett, M.J. (2009) Gibberellin

signaling in the endodermis controls Arabidopsis root meristem size. *Curr. Biol.* **19**, 1194-1199.

Verbelen, J.P., De Cnodder, T., Le, J., Vissenberg, K. and Baluska, F. (2006) The root apex of *Arabidopsis thaliana* consists of four distinct zones of growth activities: meristematic zone, transition zone, fast elongation zone and growth terminating zone. *Plant Sig. Behav.* **1**, 296-304.

Yanagi, K., Mizuno, T., You, Z. and Hanaoka, F. (2002) Mouse geminin inhibits not only Cdt1-MCM6 interactions but also a novel intrinsic Cdt1 DNA binding activity. *J. Biol. Chem.* **277**, 40871-40880.

Figure legends

Figure 1. Expression patterns of *pCDT1a::CDT1a-GUS* (a-e) and *pCDT1a::GUS* (f-j). One-DAG (a, f) and 2-DAG (b, g) seedlings, young leaves of 6-DAG seedlings (c and h), trichomes of 30-DAG seedlings (d and i), and lateral root primordia of 10-DAG seedlings (e and j). Bars = 500 μm (a-c, f-h), 10 μm (d and i), and 100 μm (e and j).

Figure 2. Expression patterns of *CDT1a* reporter genes in the root tip. (a) Diagram of GUS fusion constructs. For translational fusions, *CDT1a* coding regions were fused in-frame to the *GUS* gene (gray boxes). The open boxes indicate exons. Numbers indicate nucleotide positions from the start codon. Cy, Cy motif (blue arrowheads); D-box, destruction box (pink arrowheads); PEST, PEST domain (green boxes). (b to f) GUS staining of root tips of 3-DAG reporter lines. *pCDT1a::CDT1a-GUS* (b), *pCDT1a::GUS* (c), *pCDT1a::CDT1a (C1)-GUS* (d), *pCDT1a::CDT1a (C2)-GUS* (e) and *pCDT1a::CDT1a (C3)-GUS* (f). MZ, meristematic zone; EDZ, elongation/differentiation zone. Bar = 100 μm.

Figure 3. Stability of CDT1a-GUS fusion proteins. Three-DAG seedlings were treated with DMSO or 50 μM MG132 for 4 h and stained with GUS. *pCDT1a::GUS* (a), *pCDT1a::CDT1a-GUS* (b), *pCDT1a::CDT1a (C1)-GUS* (c), and *pCDT1a::CDT1a (C3)-GUS* (d). Bar = 100 μm.

Figure 4. Functional analysis of CDT1a (C3) in yeast and plant cells. (a) Yeast

complementation assay. The *Cdt1*-defective yeast strain *cdt1-td* was transformed with an empty vector (none) or with plasmids carrying yeast *Cdt1*, full-length *Arabidopsis CDT1a*, *CDT1a (C1)* or *CDT1a (C3)*. Three colonies were grown individually in liquid medium to mid-logarithmic phase, and spotted onto a glucose-containing medium at the permissive temperature (Glc, 24°C) or onto a galactose- and tetracycline-containing medium at the restrictive temperature (Gal/Tet, 37°C). (b) DNA ploidy analysis of leaf cells. First pairs of rosette leaves were taken from 9-, 15- or 21-DAG seedlings of wild-type and *pCDT1a::CDT1a (C3)-GUS* plants, and subjected to ploidy analysis.

Figure 5. Synchronization of tobacco BY-2 cells carrying *pCDT1a::CDT1a (C3)-GUS*. BY-2 cells were synchronized with aphidicolin (a, b) or with aphidicolin and propyzamide (c, d). (a and c) Percentage of cells in G1 (blue), S (pink) or G2/M (green) was estimated by flow cytometry. (b and d) Percentage of S-phase cells (pink), mitotic index (green) and GUS activity (blue) are shown. h, hours.

Figure 6. Expression of various *CDT1a* markers. (a to d) Expression of *pCDT1a::CDT1a (C3)-GFP* (a), *pCDT1a::CDT1a-GFP* (b), *pHTR2::HTR2-GFP* (c) and *pHTR2::CDT1a (C3)-GFP* (d) in 8-DAG root tips. Propidium iodide (PI) staining was conducted to observe cellular organization (magenta). The inset in (c) shows a magnified image of one of the circled areas, which show GFP signals on segregating chromosomes at anaphase. (e) Six-DAG root tip stained with EdU (green) and PI (magenta). (f) Expression of *pHTR2::CDT1a (C3)-RFP* (magenta) and *pCYCB1::CYCB1-GFP* (green) in an 8-DAG

root tip. Here, and in (g) to (i), images of RFP and GFP fluorescence, and a merged image, are shown from left to right. (g to i) Magnified images of cells in (f) indicated by arrowheads, arrows and squares, respectively. Bars = 50 µm (a to f) and 10 µm (g to i).

Figure 7. Time-lapse imaging of cell cycle progression in the root meristem. Epidermal cells in the root meristem were observed for 5-DAG seedlings harboring both *pCYCB1::CYCB1-GFP* and *pHTR2::CDT1a (C3)-RFP*. A single nucleus was traced sequentially over the indicated time period. (a) Fluorescence images on the GFP-based timescale. The time when GFP-labeled chromosomes were aligned on the equatorial plane was set to zero. (b) Fluorescence images on the RFP-based timescale. The time when the intensity of RFP signals first exceeded twice the value detected 2 h previously was set to zero. Bars = 5 µm. (c and d) Fluorescence intensity of GFP (green) and RFP (pink). Brightness in the nuclear area was quantified using Olympus FV10-ASW software. The time scale was based on GFP (c) or RFP (d). Note that the data are displayed at 1-h intervals, but with 10-min intervals from -60 min to 60 min on the GFP-based time scale (a and c) because GFP fluorescence changed rapidly during this period. Error bars represent the standard deviation. n = 25 (c) and 15 (d).

Figure 8. Schematic representation of cell cycle progression in the *Arabidopsis* root epidermis. The duration of each stage displaying GFP (green) and/or RFP (magenta) fluorescence, or lacking either, was estimated by time-lapse imaging of the *Arabidopsis* root meristem using the Cytrap system.

Figure 9. Expression of the Cytrap markers around the transition zone of *Arabidopsis* root. Expression of *pHTR2::CDT1a (C3)-RFP* (magenta) and *pCYCB1::CYCB1-GFP* (green) was observed with 13-DAG seedlings. (b) is a magnified image of the boxed area in (a). Arrowheads indicate the boundaries between the meristematic zone (MZ), the transition zone (TZ) and the elongation/differentiation zone (EDZ). Bars = 100 μm.
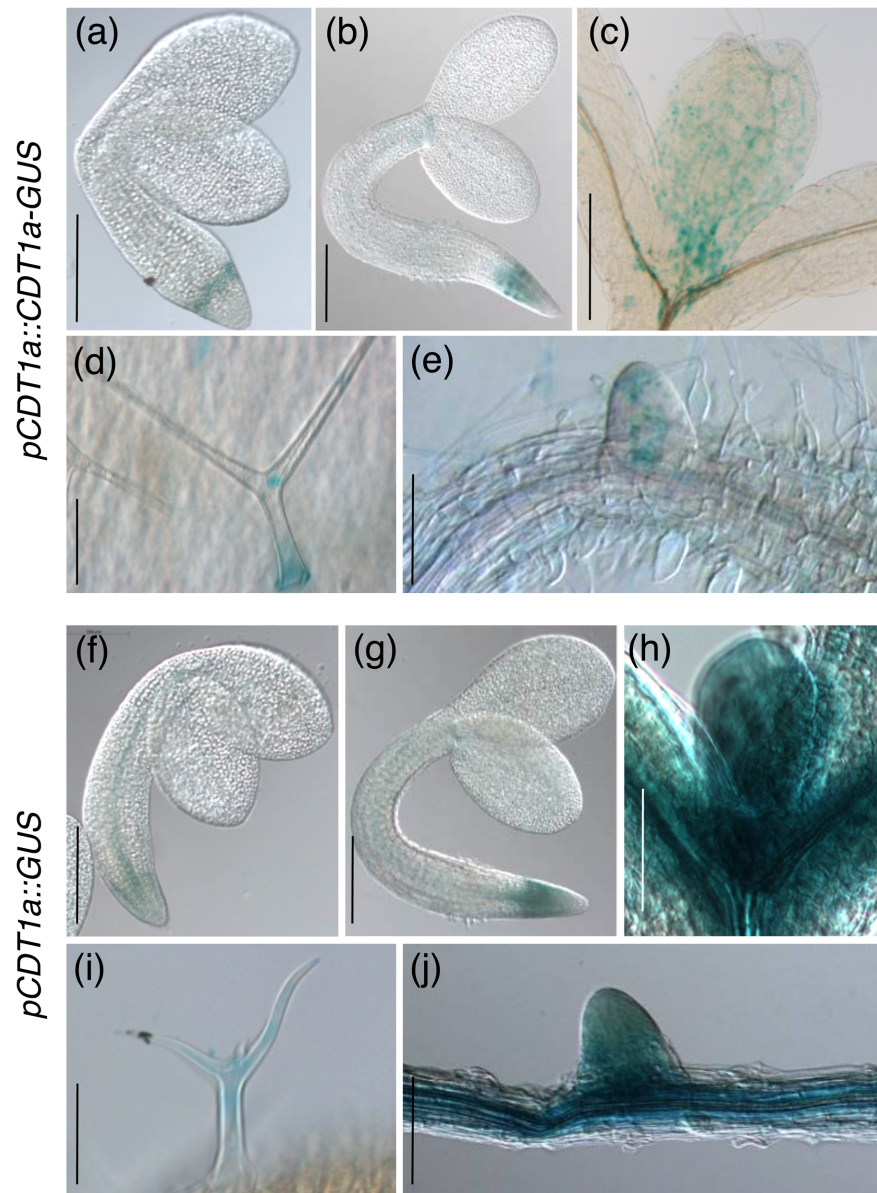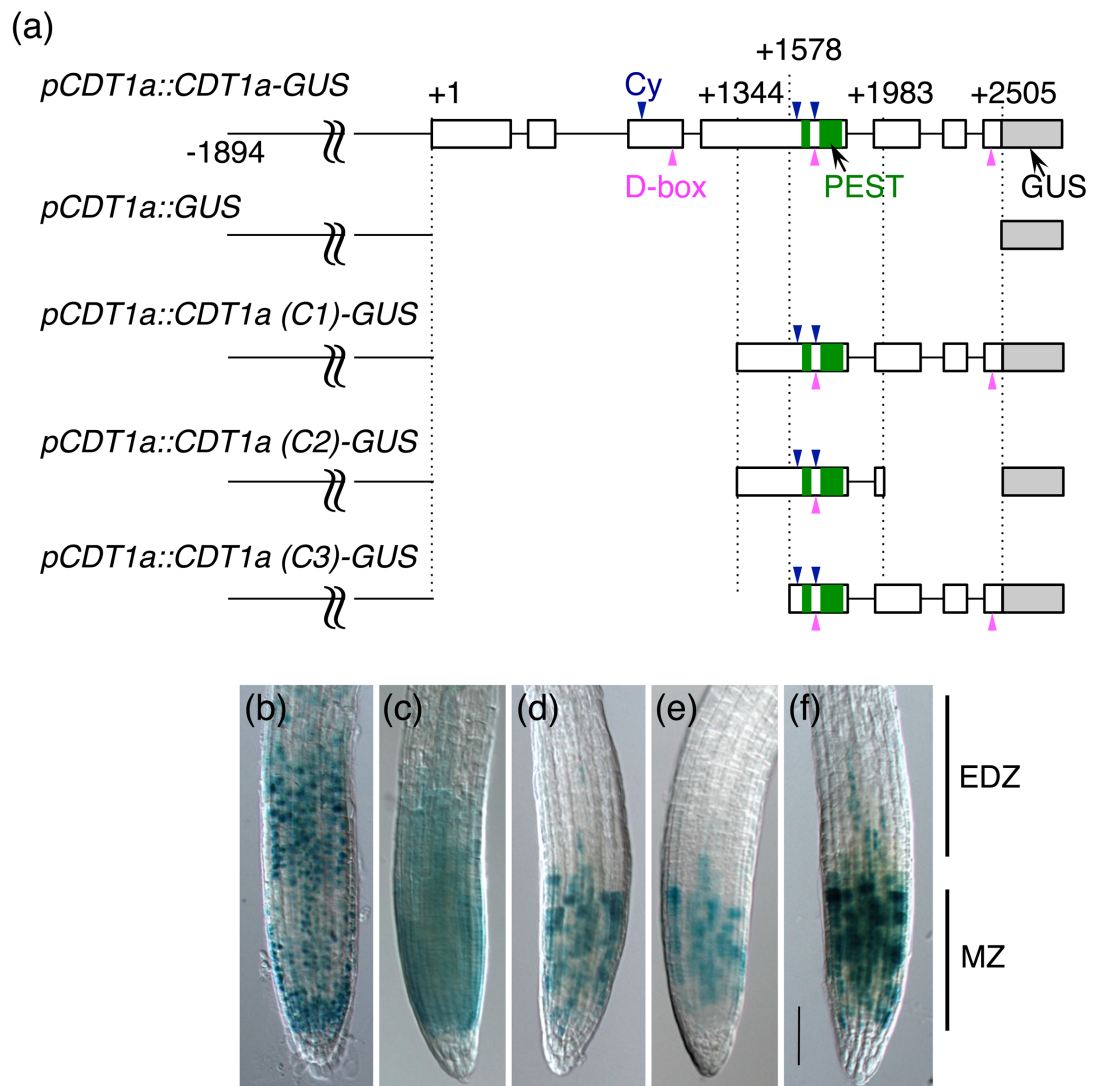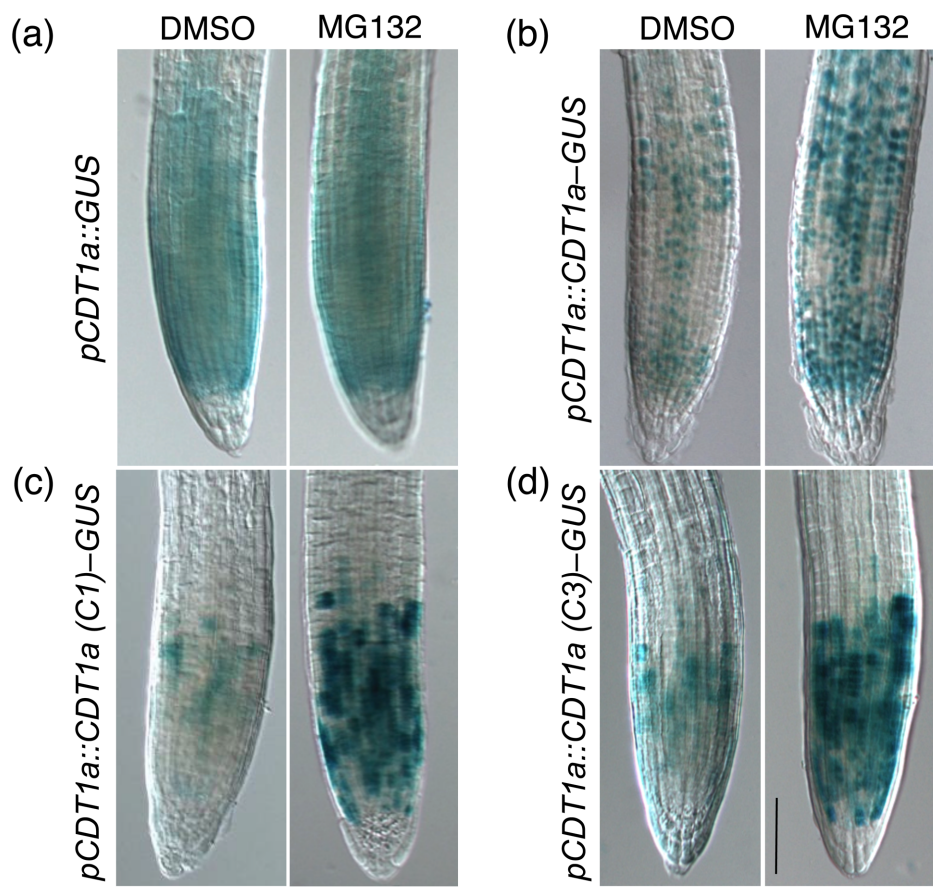
pCDT1a::CDT1a-GUS

pCDT1a::GUS

Figure 1

Figure 2

Figure 3
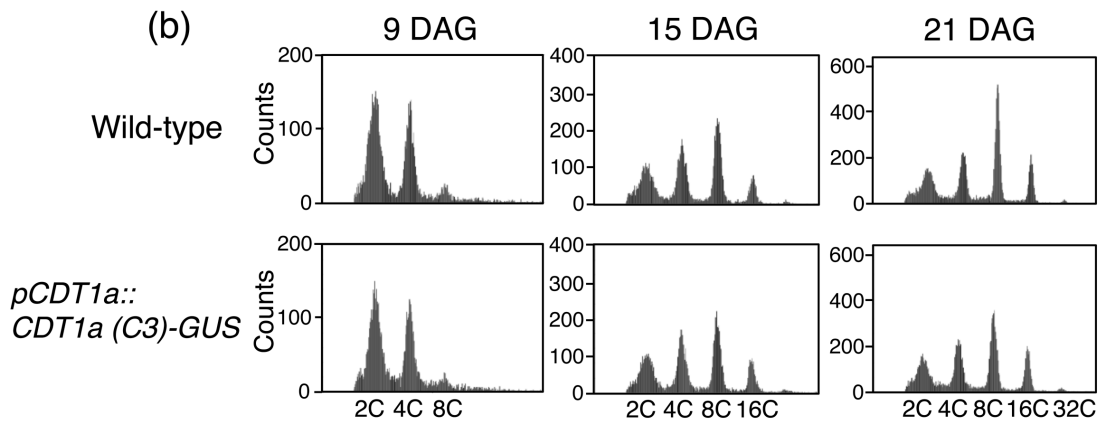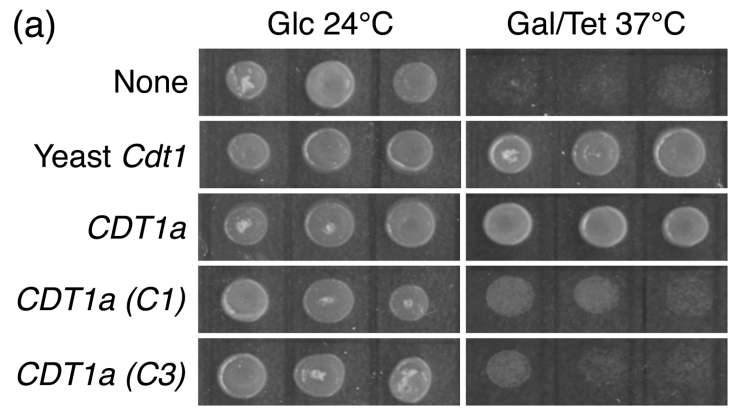
Figure 4
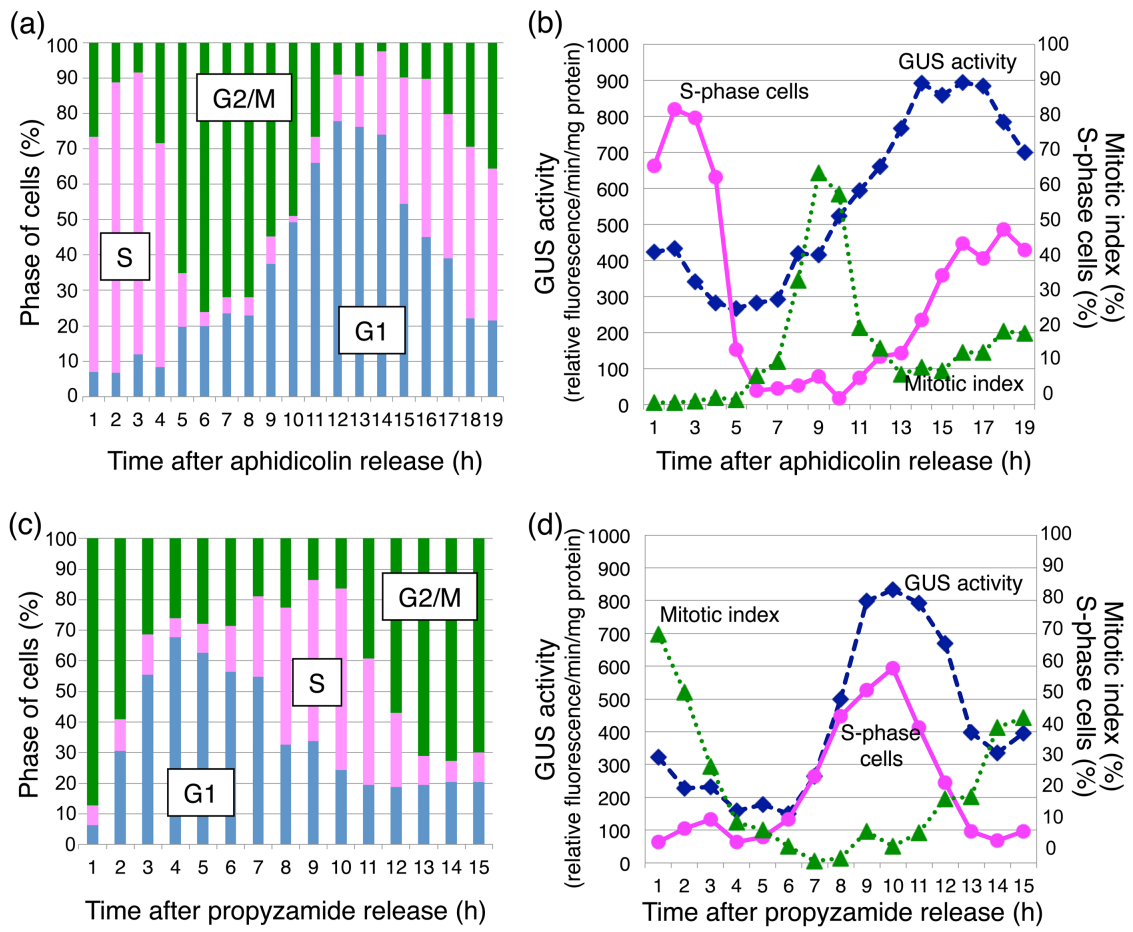
Figure 5
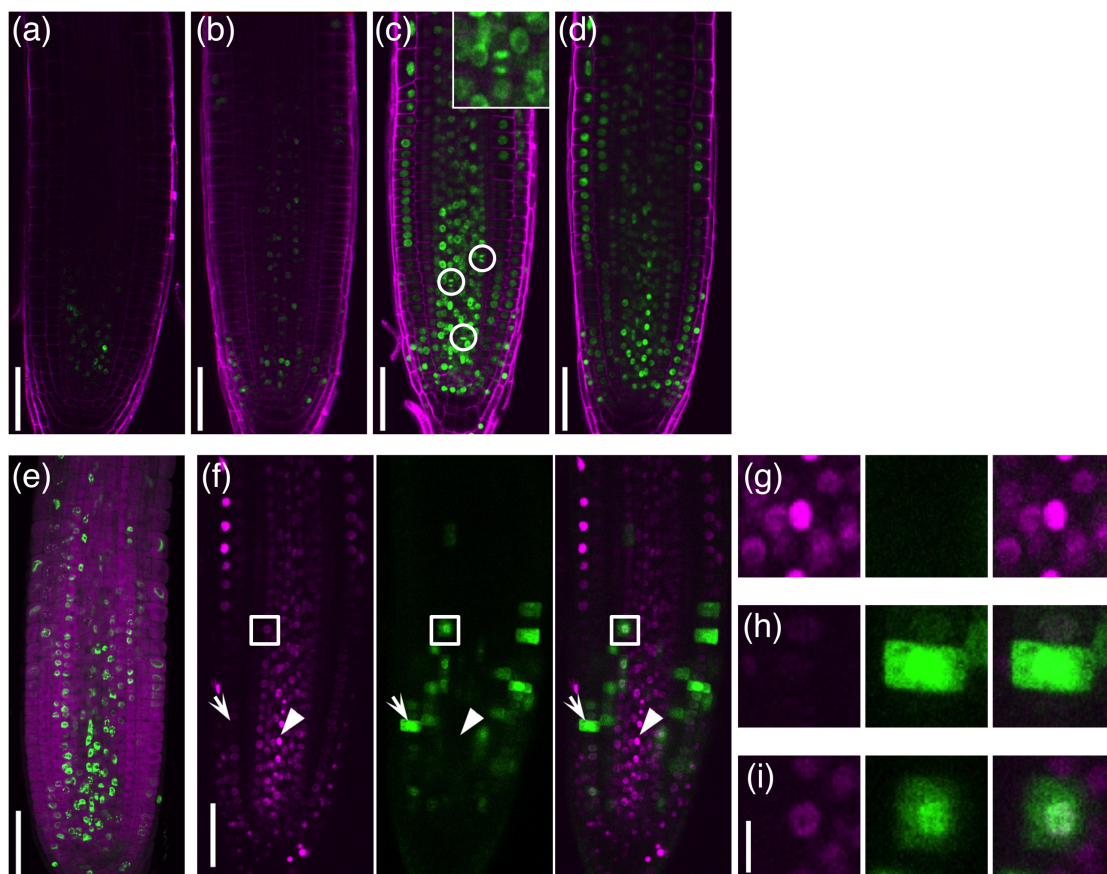
Figure 6

Figure 7

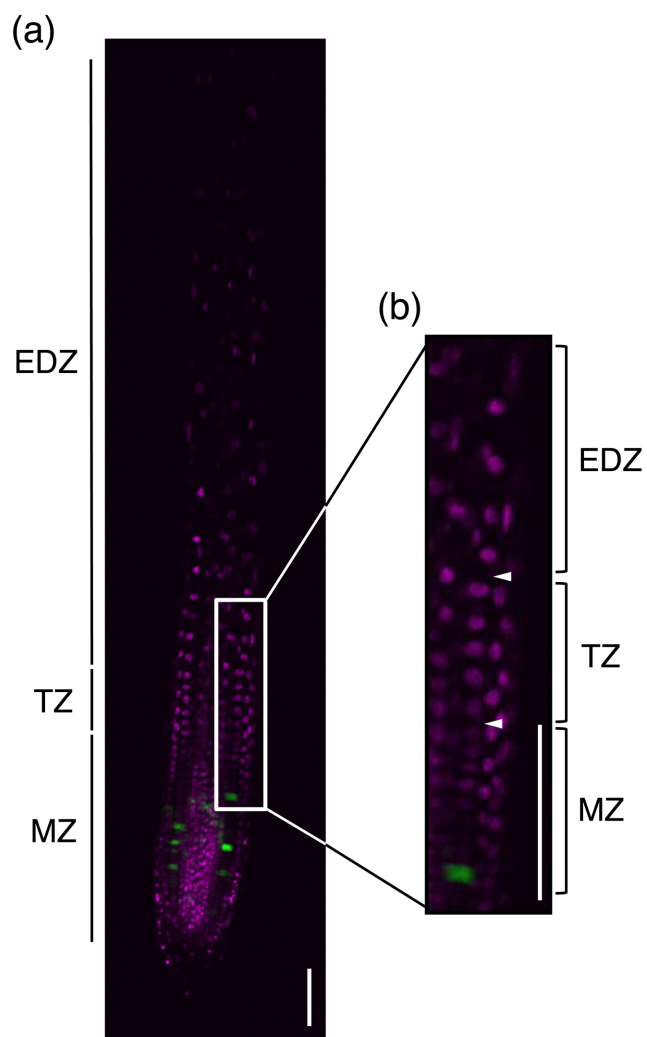**Figure 8**

(a)

EDZ

TZ

MZ
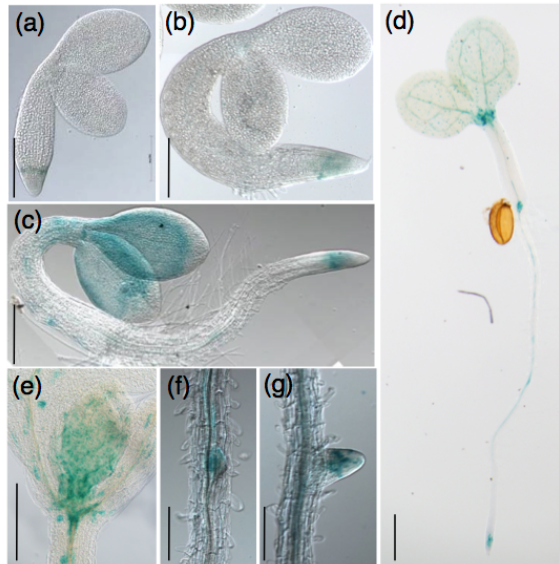
(b)

EDZ

TZ

MZ
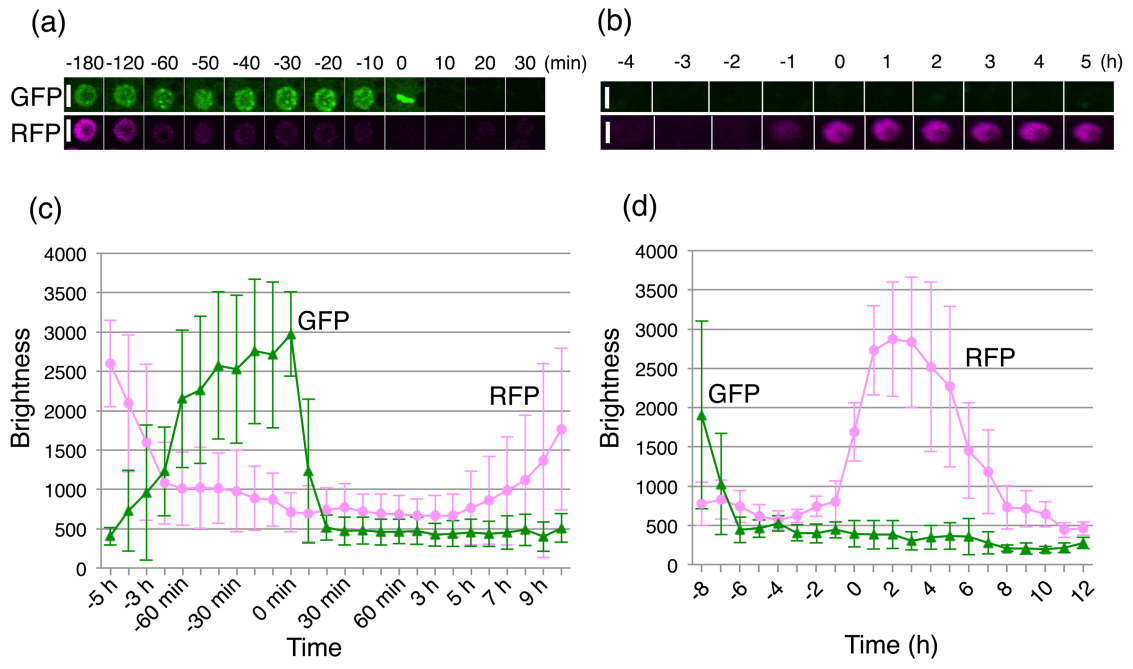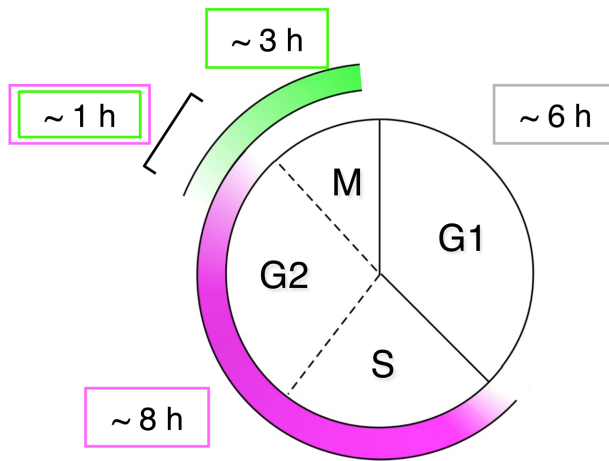
Figure 9

Figure S1.

Expression pattern of *pCDT1a::CDT1a (C3)-GUS*. One-DAG (a), 2-DAG (b), 3-DAG (c) and 4-DAG (d) seedlings, and young leaves of 5-DAG seedlings (e) and emerging lateral roots (f and g). Bars = 500 μm (a-e) and 100 μm (f and g).
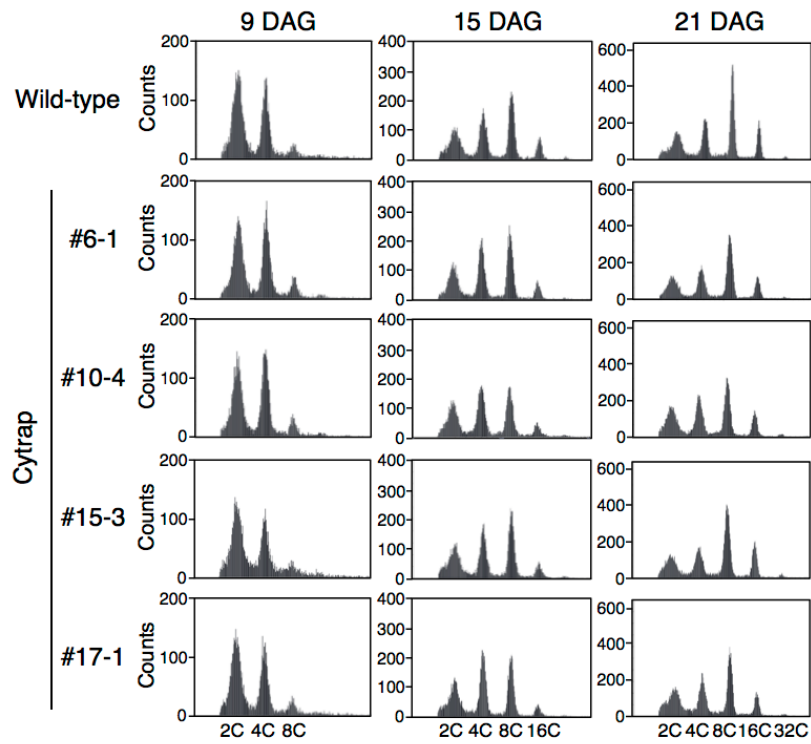
Figure S2.

DNA ploidy analysis of leaf cells of Cytrap transgenic lines. First pairs of rosette leaves were taken from 9-, 15- or 21-DAG seedlings of wild-type and four independent Cytrap transgenic lines (#6-1, #10-4, #15-3 and #17-1), and subjected to ploidy analysis.